Concentration sensor based on circular lattice photonic crystal fiber placed between two single mode fibers

ABHINAV BHATNAGAR*, NIDHI SINGH
School of Electrical, Electronics and Communication EnggGalgotias University, Plot No. 2, Sector 17-A, GautamBudh Nagar Yamuna Express Way, GREATER NOIDA - 201 301 (UP) India

In this paper, we have proposed a novel concentration sensor using circular lattice photonic crystal fiber (PCF) sandwiched in between two single mode fibers (SMF). For simulating this, 1 μm length PCF of circular lattice is placed between two SMF having length 1 μm length each. To provide better coupling between SMF and PCF, the diameters of the core are made equal. The input is fed at one end and the output is analysed at another end with respect to different concentrations of alcohol in the air holes of PCF using Finite Difference Time Domain (FDTD) method. The output at the end of the sensor shows that the variation of electric field intensity is linear with respect to concentration of alcohol.

(Received January 24, 2016; accepted November 25, 2016)

Keywords: FDTD Method, Single mode fiber, Photonic crystal fiber, Concentration sensor

1. Introduction

Photonic crystals structures (PCS) and fibers have achieved a lot of research significance due to their projected applications in various fields [1-2]. They are becoming popular as sensors due to their well-defined physical properties such as reflectance, transmittance and high levels of sensitivity resulting in precise detection limits as well as due to the sparkling visual quality they display in the visible range of wavelengths. When the photonic crystal technology is employed the sensor itself is very small and measurements are possible through coupling the incident and reflected/transmitted light to optical fibers and analyzing them in remote locations [3]. Sensors based on PCS are gaining interest since last decade. The reason is the increasing demand of research in this area is due to flexibility of PCS in tailoring different optical properties as per the desired requirement. Photonic crystals with two dimensional structures have been extensively studied for their possible use in different sensing applications [2-3]. Many researchers have investigated PCS application in sensing such as pressure, strain, temperature, corrosion, etc. To accompany the wide use of PCS as the sensing element, recently PCF has also attracted great interest in the sensing field. In this paper we proposed a novel concentration sensor based on PCF. The sensors based on PCS have some limitation in fabrication. This is achieved by placing the PCS-2D between two glass slides [3-5] before incident signal is allowed to pass through it. But in this proposed design a circular PCF is placed between two single mode fibers this solves three problems: First, no extra coupling is needed from source to the sample is avoided; second transmission efficiency in this case would be better than previous method [3]. Third, circular lattice PCF has an advantage over other lattice structures such as hexagonal lattice structure that it facilitates comparatively easy fabrication [6].

2. Theory

FDTD SOLUTION:

FDTD method was first proposed by Kane S. Yee in the year 1966 to analyze the scattering of an electromagnetic wave by a perfectly conducting cylinder. The method solves the Maxwell's time dependent curl equation by first converting them to finite difference equations. Maxwell's equations in an isotropic medium [7] are:

$$\frac{\partial \mathrm{B}}{\partial \mathrm{t}} + \nabla \times \mathrm{E} = 0 \tag{1}$$

$$\frac{\partial \mathrm{D}}{\partial \mathrm{t}} - \nabla \times \mathrm{H} = 0 \tag{2}$$

$$\mathrm{B} = \mu \mathrm{H} \tag{3}$$

$$\mathrm{D} = \epsilon \mathrm{E} \tag{4}$$

whereJ, μ, and ∈are assumed to be given functions of space and time. In a rectangular coordinate system, (l) and (2) are equivalent to the following system of scalar equations:

$$-\frac{\partial \mathrm{B_x}}{\partial \mathrm{t}} = \frac{\partial \mathrm{E_z}}{\partial \mathrm{y}} - \frac{\partial \mathrm{E_y}}{\partial \mathrm{z}}, \tag{5}$$

$$-\frac{\partial B_y}{\partial t} = \frac{\partial E_x}{\partial z} - \frac{\partial E_z}{\partial x}, \quad (6)$$

$$\frac{\partial B_z}{\partial t} = \frac{\partial E_x}{\partial y} - \frac{\partial E_y}{\partial x}, \quad (7)$$

$$\frac{\partial D_x}{\partial t} = \frac{\partial H_z}{\partial y} - \frac{\partial H_y}{\partial z} - J_x, \quad (8)$$

$$\frac{\partial D_y}{\partial t} = \frac{\partial H_x}{\partial z} - \frac{\partial H_z}{\partial x} - J_y, \quad (9)$$

$$\frac{\partial D_z}{\partial t} = \frac{\partial H_y}{\partial x} - \frac{\partial H_x}{\partial y} - J_z, \quad (10)$$

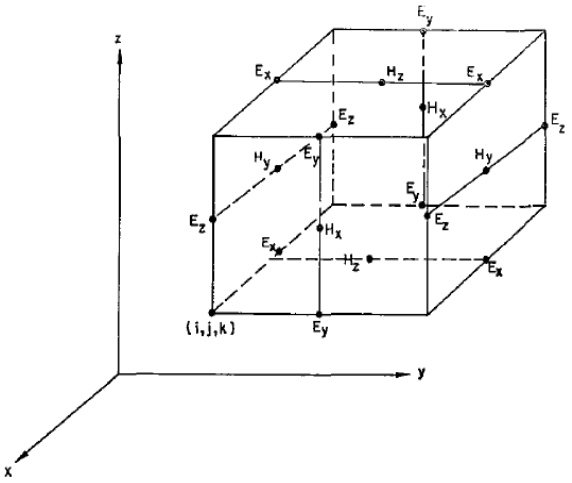

Fig.1. Grid points of E and H field components

Grid point in space is defined as

$$(i, j, k) = (i\,\Delta x, j\,\Delta y, K\,\Delta z) \quad (11)$$

$$F(i\Delta x, j\Delta y, k\Delta z, n\Delta t) = F^n(i, j, k) \quad (12)$$

For a perfectly conducting boundary equation (5) becomes

$$\frac{B_x n+1/2\left(i,j+\frac{1}{2},k+\frac{1}{2}\right) - B_x n-1/2\left(i,j+\frac{1}{2},k+\frac{1}{2}\right)}{\Delta t} = \frac{E_y n\left(i,j+\frac{1}{2},k+1\right) - E_y n\left(i,j+\frac{1}{2},k\right)}{\Delta z} - \frac{E_z n\left(i,j+1,k+\frac{1}{2}\right) - E_z n\left(i,j,k+\frac{1}{2}\right)}{\Delta y} \quad (13)$$

The finite difference equations can be constructed in the same manner for equation (6) and (7). For equation (8):

$$\frac{D_x n\left(i+\frac{1}{2},j,k\right) - D_x n-1\left(i+\frac{1}{2},j,k\right)}{\Delta t} = \frac{H_z n-1/2\left(i+\frac{1}{2},j+\frac{1}{2},k\right) - H_z n-1/2\left(i+\frac{1}{2},j-\frac{1}{2},k\right)}{\Delta y} - \frac{H_y n-1/2\left(i+\frac{1}{2},j,k+\frac{1}{2}\right) - H_y n-1/2\left(i+\frac{1}{2},j,k-\frac{1}{2}\right)}{\Delta z} + j_x n-1/2\left(i+\frac{1}{2},j,k\right) \quad (14)$$

The finite difference equations for equation (9) and (10) can be written in the same manner, respectively. E-field and the H-field grid points chosen are shown in Fig. 1

BOUNDARY CONDITIONS

The boundary conditions are taken to be perfectly conducting which implies that there is no reflection of electromagnetic waves at the surface that is the tangential component of electromagnetic field is zero [7]. For computational stability the grid size and stability is given by relation:

$$\sqrt{(\Delta x)^2 + (\Delta y)^2 + (\Delta z)^2} > c\Delta t = \sqrt{\frac{1}{\epsilon\mu}}\Delta t, \quad (15)$$

where c = velocity of light,

Similarly Maxwell's equations in 2-D can be derived and can be solved for various Electric field and magnetic field points by converting them into finite difference equations. Thus to solve these equations we have employed FDTD solution from Lumerical to simulate light propagation through a combination of three different dielectric layers with the use of Gaussian source using boundary condition as Perfectly Matched Layer (PML). Only 1 μm of dielectric layer is considered for this simulation due to the memory constraint. However with the increase in memory the sensor dimension can be extended to few centimeters [7].

Design:

The cross sections of PCF and SMF, taken for our investigation are shown in Fig. 2.

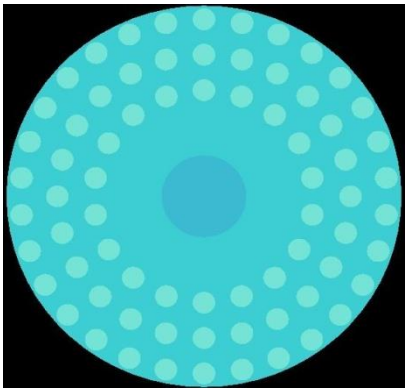

Fig. 2. Cross section of PCF, with circular lattice of constant a = 0.13 µm, radius of air hole = 0.04 µm and core radius r = 0.15 µm, refractive Index of the core = 1.45 and of cladding= 1.43

A 1 µm gap is formed initially in between two SMF of length 1 µm each. Then PCF of circular lattice of 1 µm length is injected with the alcohol in to the air holes is placed in the gap. The PCF is placed such that no air gap is left at the interface of SMF and PCF. The design proposed is shown in Fig. 3.

Fig. 3.Proposed design of the sensor. I/P is the input where the signal is fed into the sensor and O/P is the output where the signal is analyzed

FDTD Simulation and Analysis:

To simulate the field intensity for a given concentration alcohol filled in PCF, across the output for given input, we use the data from reference [3] shown in Table 1. FDTD simulation is used to get the field distribution at the output, for a given refractive index at the holes of PCF.

Table 1. Variation of E- field intensity with change in concentration of alcohol

S. no.	Concentration in g/ml	Refractive Index, n	Electric Field Intensity in V/m
1	5	1.34313	0.375006
2	10	1.34721	0.374744
3	15	1.35420	0.374296
4	20	1.36051	0.373890
5	40	1.36271	0.373749

The simulated field for one particular value of concentration is shown in the Fig. 4.

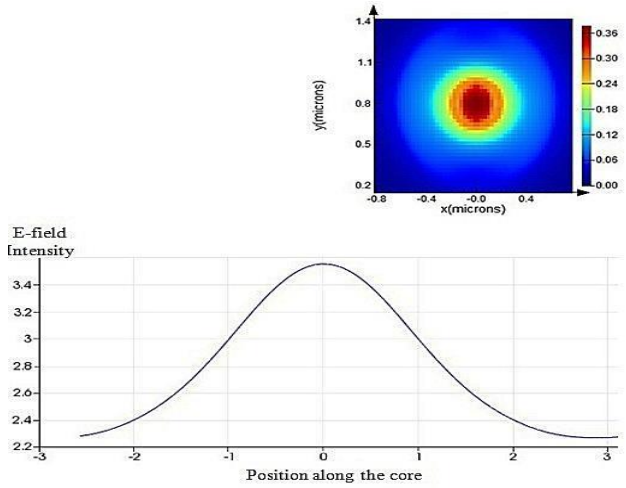

Fig. 4. Electric field variation due to different concentration in the air holes of PCF.

The graph shows electric field distribution obtained at output of the fiber for 15 g/ml concentration. Similarly for other concentration values, the Electric field value is obtained and analyzed. The wavelength of the signal is maintained at the third window *i.e.*, 1550 nm. We found that the distribution at the output is somewhat similar to the input, but as the concentration is increased the refractive index changes, the electric field intensity at the output end also changes. The simulation results are shown in Fig. 4, which shows the variation of the electric field intensity along the cross section of fiber. The variation of electric field intensity with the change of dielectric constant can be explained as follows: since the refractive index of the alcohol filling the air gap in PCF changes, photonic band gap (PBG) of the structure also changes [9]-[10]. The total power transmitted through the sensor depends on this PBG. Thus there is a variation of input electric field intensity with the change of refractive index.

However, for sensing application this change of electric field must vary linearly. To represent this we plot a graph between refractive index and corresponding field at the axis across the output as in Fig. 5. The linear variation of the electric field intensity shows that concentration can be measured more accurately using this principle. The investigation can also be done here for larger dimension with extended length of PCF, using improved computational facilities.

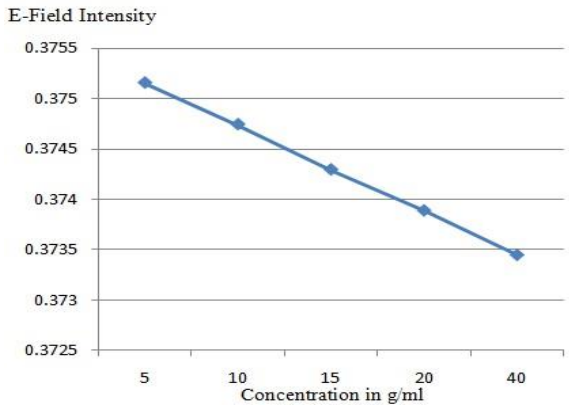

Fig. 5. Plot showing electric field versus concentration at the output of fiber

3. Conclusion

We demonstrate the use of short length circular lattice PCF placed between two SMF for measuring concentration of alcohol using FDTD method. It is found that a combination of SMF- PCF-SMF system really can be used as a better sensing device owing to its perfect linear variation of electric field with concentration. The similar results are obtained from the hexagonal lattice PCF also [3]. The use of circular lattice PCF has an advantage that it is relatively easy to fabricate [8]. PCS fibers and gratings have achieved a lot of research significance due to their projected applications in various fields [12-13]. However it is found that within the C-band the practical applications are limited due to higher dispersion losses [11].

Acknowledgment

The authors acknowledge the support provided by Dean Academics and Dean SEECE, Galgotias University.

References

[1] Rajesh V. Nair, R. Vijaya, Progress in Quantum Electronics **34**(3), 89 (2010).
[2] E. Yablonovitch, Physical Review Letters **58**(20), 2095 (1987).
[3] G. Palai, S. K. Tripathy, Optics Communications **285**(10-11), 2765 (2012).
[4] I. A. Sukhoivanov, I. V. Guryev, Springer, 2009, Chapter 6.
[5] S. K. Tripathy, S. P. Dash, S. Sahu, C. Mohapatro, Optics Communications **285**(13-14), 3234 (2012).
[6] C. Gui, J. Wang, in IEEE Photonics Journal **4**(6), 2012 (2152).
[7] Kane Yee, in IEEE Transactions on Antennas and Propagation **14**(3), 302 (1966).
[8] A. V. Dyogtyev, I. A. Sukhoivanov, R. M. De La Rue, Journal of Applied Physics **107**, (2010).
[9] R. T. Bise, R. S. Windeler, K. S. Kranz, C. Kerbage, B. J. Eggleton, D. J. Trevor, Optical Fiber Communication Conference 466 (2002).
[10] Kurt Busch, Sajeev John, Phys. Rev. Lett. **83**, 967 (1999).
[11] ParthaSonaMaji, Partha Roy Chaudhuri, ISRN Optics **2013**, Article ID 986924, 9 pages, 2013.
[12] Nidhi, Umesh Tiwari, NishthaPanwar, R. S. Kaler, Randhir Bhatnagar, Pawan Kapur, IEEE Sensors Journal **13**(11), 4139 (2013).
[13] Nidhi, R.S. Kaler, Pawan Kapur, J. Optoelectron. Adv. M. **8**(1-2), 45 (2014).

*Corresponding author: abhinav.jrf@mnit.ac.in